Polymeric Nanoparticle Preparation that Eradicates Tumors

ARTICLE *in* NANO LETTERS · JANUARY 2006

Impact Factor: 13.59 · DOI: 10.1021/nl0519229 · Source: PubMed

4 AUTHORS, INCLUDING:

Christian Brueckner
University of Connecticut
149 PUBLICATIONS **3,599** CITATIONS

SEE PROFILE

NANO LETTERS

2005
Vol. 5, No. 12
2552−2556

Polymeric Nanoparticle Preparation that Eradicates Tumors

Jason R. McCarthy,[†,§] J. Manuel Perez,[†,§,||] Christian Brückner,[‡] and Ralph Weissleder*[,†]

MGH-Harvard Medical School, Center for Molecular Imaging Research, 149 13th Street, Room 5404, Charlestown, Massachusetts 02129, and Department of Chemistry, University of Connecticut, 55 North Eagleville Road, Storrs, Connecticut 06269

Received September 28, 2005; Revised Manuscript Received October 24, 2005

ABSTRACT

We report the production of poly(lactic-*co*-glycolic acid) nanoparticles that encapsulate the photosensitizer *meso*-tetraphenylporpholactol. These nanoparticles are stable and nonphototoxic upon systemic administration. Upon cellular internalization, the photosensitizer is released from the nanoparticle and becomes highly phototoxic. Irradiation with visible light results in cell-specific killing of several cancer cell lines. Importantly, in vivo experiments show complete eradication of cancers in mouse models. The concept of photosensitizers with selective phototoxicity should have widespread applications in cancer therapy.

Photosensitizers are capable of producing cytotoxic singlet-oxygen when irradiated with light of the appropriate wavelength.[1] When this process occurs within cells, it can result in irreversible damage to cellular components leading to cell death. Compared to porphyrins, chlorins offer increased absorption of the farthest-red sideband, higher singlet oxygen quantum yields, and greater depth of penetration of light, making them overall better photosensitizers and attractive for use in photodynamic therapy (PDT).[2,3] However, most of the current photosensitizing agents have relatively narrow therapeutic windows and are associated with significant side effects, such as photosensitivity upon exposure to sunlight due to skin accumulation.[4] Recent strategies to improve their efficacy include tumor targeting using peptide conjugates and antibodies[5] or encapsulation within nanoparticles[6] to yield higher local concentrations at therapeutic sites. The rationale for nanoparticle encapsulation is that typically hydrophobic photosensitizers will be protected from the aqueous environment, thereby reducing aggregation, a process that results in decreased singlet oxygen quantum yields.[7] Nanoparticles also have the advantage of long blood half-lives and increased uptake by tumor tissue via the enhanced permeability and retention effect.[8] Nanoparticles reported previously, however, were intrinsically phototoxic.

We hypothesized that nanoparticles could be devised in such a manner that the excited states of the photosensitizer would be quenched and thus be used as an activatable PDT nanoagent with improved therapeutic properties. In the present study, we have utilized a chlorin, *meso*-tetraphenylporpholactol (**4**),[3] the polarity of which is ideal for nanoparticle preparation, that aggregates upon encapsulation, causing efficient quenching of the chromophore excited states. This design is counter to those described previously (vide supra) because aggregation of the photosensitizer within the particle is beneficial, not detrimental. Using poly(lactic-*co*-glycolic acid) (PLGA, 50:50)[9] as base material, we show that the excited states of the chlorin analogue, **4**, are quenched completely and therefore unable to fluoresce or induce phototoxicity. Upon cell internalization it regains its ability to fluoresce and produce singlet oxygen, resulting in an activatable PDT-nanoagent. Results are compared to those obtained by encapsulating *meso*-tetraphenylporphyrin (**1**). The nanoparticle matrix (PLGA) was chosen for its biocompatibility and current clinical use.[9]

Scheme 1 shows the synthesis of *meso*-tetraphenylporpholactol **4**, from *meso*-tetraphenylporphyrin (TPP, **1**). The OsO_4-mediated dihydroxylation of **1** produces the *vic*-diol chlorin, *meso*-tetraphenyl-2,3-dihydroxychlorin **2**,[10] whereas permanganate oxidation of the diol moiety in **2** generates porpholactone **3**.[11] Finally, reduction of the Zn(II) chelate of **3** with DIBAL-H, followed by removal of the central metal ion yields *meso*-tetraphenylporpholactol **4**.[3] The UV−vis

* Corresponding author. Center for Molecular Imaging Research, Massachusetts General Hospital and Harvard Medical School, Building 149, 13th Street, Room 5403, Charlestown, MA 02129. Fax: 617-726-5708. Ph: 617-726-8226.

† MGH-Harvard Medical School.

‡ University of Connecticut.

§ These authors contributed equally to this work.

|| Current address: University of Central Florida, Nanoscience Technology Center, 12424 Research Parkway, Suite 400, Orlando, FL 32826.

10.1021/nl0519229 CCC: $30.25
Published on Web 11/12/2005

Scheme 1. Synthesis of *meso*-Tetraphenylporpholactol **4** from TPP **1**[a]

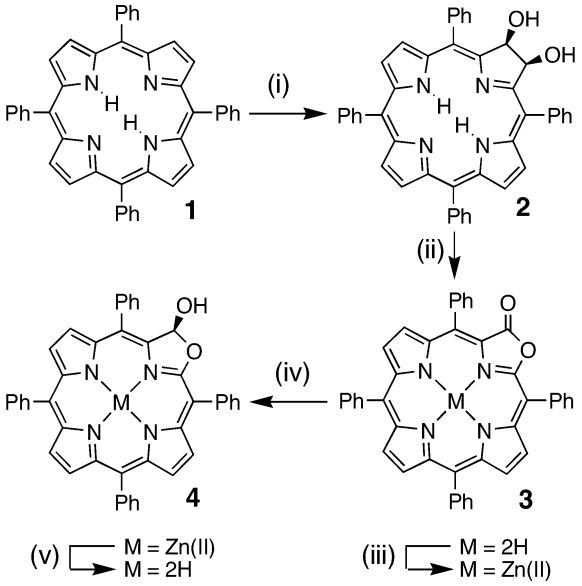

[a] Reaction Conditions: (i) 1. OsO_4, 2:1 $CHCl_3$:pyridine, 2. H_2S;[10] (ii) $KMnO_4$, 18-crown-6;[11] (iii) $Zn(OAc)\cdot 2H_2O$, DMF; (iv) 1. DIBAL-H, THF, 2. H_2O; (v) 6 M HCl.[3]

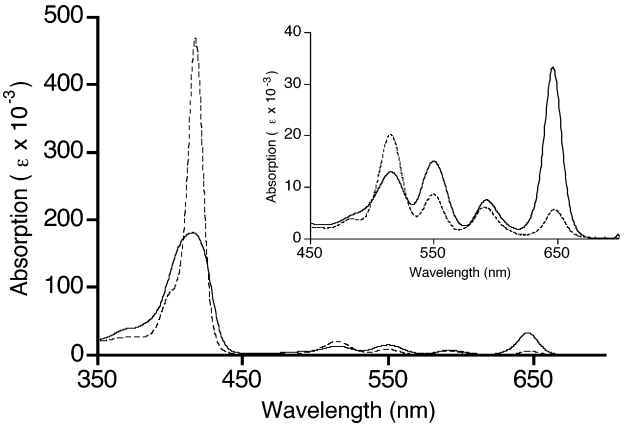

Figure 1. UV−vis absorption spectra of **1** (- - -) and **4** (—) in CH_2Cl_2. Inset: Expanded view of the sideband region of the UV−vis absorption spectra.

Table 1. Photophysical Properties of Porphyrin and Chlorins Used in This Study[a]

	ϵ ($L\ mol^{-1}cm^{-1}$)	ϕ_{Fl}	ϕ_{Δ}
1	3.4×10^3	0.04	0.64
4	3.2×10^4	0.16	0.85

[a] ϵ calculated at 646 nm; ϕ_{FL} = fluorescence quantum yield ± 0.02 (in air-saturated acetone); ϕ_{Δ} = singlet oxygen quantum yield ± 0.07 (in air-saturated DMF).

spectra of **1** and **4** are shown in Figure 1, and their corresponding photophysical properties are summarized in Table 1. As compared to porphyrin **1**, porpholactol **4** possesses a 10-fold higher extinction coefficient of the farthest-red sideband at 646 nm, and a higher singlet oxygen quantum yield (Φ_{Δ}), making it an overall better photosensitizer. In addition, porpholactol **4** has a higher fluorescence quantum yield (Φ_{FL}) than **1**; thus, its in vivo biodistribution could be monitored by fluorescence imaging prior to light therapy.[12] Although lipophilic photosensitizers have shown increased biological activity versus hydrophilic analogues,[13] the main drawback of these photosensitizers is a lack of aqueous solubility, which renders them useless for clinical applications without proper formulation.

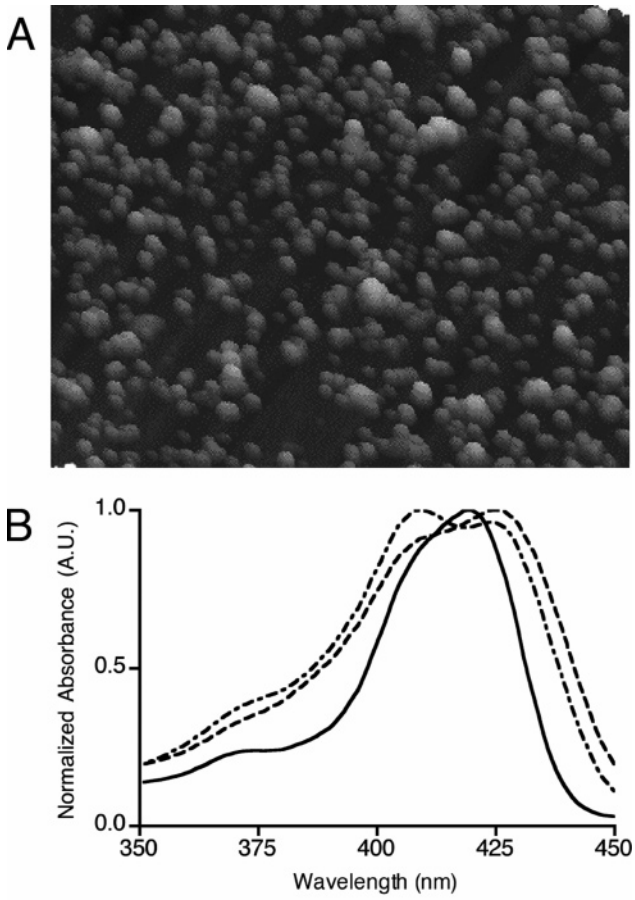

Figure 2. (A) Representative atomic force microscopy image (4 × 3 μm^2 field of view) of nanoparticles **n4** encapsulating porpholactol **4**. (B) Soret band region of **4** in DMF (—), **4** in DMF/H_2O (1:2) (- - -), and **n4** in H_2O (—·—·) illustrating the aggregation of **4** in **n4** nanoparticles.

The polymeric nanoparticles encapsulating porphyrin **1** or porpholactol **4** were produced via a solvent-diffusion method to result in nanoparticles **n1** and **n4**, respectively. Slow addition of a polymer−photosensitizer solution in DMF allows for diffusion of the solvent into the water, resulting in the formation of a slightly opaque, colored, aqueous suspension of porphyrin-PLGA nanoparticles. The nanoparticles were purified and isolated by dialysis followed by filtration (0.1-μm cutoff). This method produces nanoparticles with smaller particle sizes than most current methods and avoids the use of surfactants and emulsifiers. The presence of nanoparticles was verified by atomic force microscopy (AFM, Figure 2A). Particle size distribution, determined by light scattering, shows a narrow distribution with a mean diameter of 58 nm (polydispersity index = 0.12) for **n1**, and 98 nm (polydispersity index = 0.10) for **n4**, that

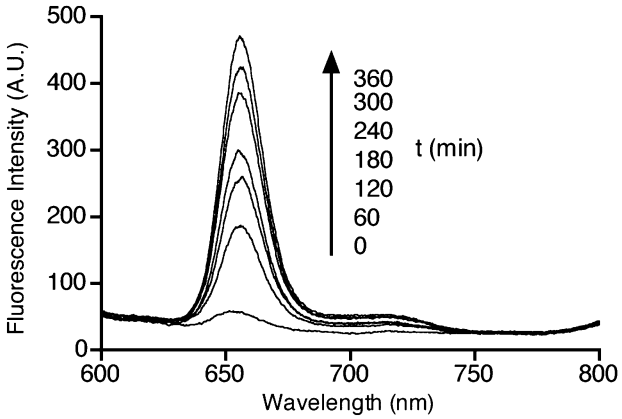

Figure 3. Time-dependent increase in fluorescence of **n4** nanoparticles (300 nM) in an aqueous solution containing lipid (0.5% intralipid) illustrating the time-dependent release of **4**.

is reproducible between preparations to ±5 nm. Nanoparticles under 100 nm, similar in size to most viruses, are particularly suitable as target-specific nanoagents for imaging and therapeutic applications.[14] The observed difference in size between the two preparations appears to depend on the photosensitizer used because other variables such as the initial polymer-to-photosensitizer ratio, vortexing and addition rates, and solution volumes, were held constant. Once purified, the aqueous nanoparticle preparation is stable, without significant loss of activity or change in size when stored in the dark at room temperature for 6−12 months, as has been reported previously for similar porphyrin nanoparticle preparations.[15] The reason for this stability is not well understood, but may be due to the presence of an extremely hydrophobic photosensitizer in the core of the nanoparticle, which decreases the rate of hydrolysis of the polymer as a result of the nonfavorable interactions with the surrounding medium.

Next, we determined the percent loading (mass of photosensitizer/mass of nonoparticles) of photosensitizer in the nanoparticles. After lyophilization of the respective nanoparticle suspension, the samples were weighed out, dissolved in methylene chloride, and the mass of photosensitizer was determined spectrophotometrically. It was found that both **n1** and **n4** had similar photosensitizer loading, 10% and 12%, respectively. The concentration of photosensitizer in the stock nanoparticle suspension was also determined spectrophotometrically. This was accomplished by first lyophilizing a known volume of the respective nanoparticle suspension, followed by dissolution in methylene chloride and calculation of the concentration via the Beer−Lambert law. The concentration of porphyrin in **n1** was approximately 50 μM, whereas the porpholactol in **n4** was 150 μM.

The UV−vis absorption spectra of **n1** and **n4** indicate the presence of aggregates within the particles, as shown in Figure 2B for **n4**. Upon encapsulation, the Soret band region of the spectum broadens significantly, with the appearance of two peaks, similar to those observed for a 2:1 H_2O/DMF solution of **4**.[16]

The intensity of the fluorescence emission from the photosensitizer within the nanoparticle is significantly lower than that in its free state, as is expected for aggregates. Unfortunately, because of the diffraction of light expected to be caused by the polymeric shell, the fluorescence quantum yields for **n1** and **n4** cannot be calculated accurately. Additional photophysical experiments, such as transient triplet−triplet lifetimes, fluorescence emission lifetimes, or singlet oxygen quantum yields are currently under investigation. When the nanoparticle suspension was diluted with acetone, a process that solublizes the PLGA polymeric nanoparticles and releases the photosensitizer, fluorescence intensity was completely restored. A similar effect was also observed when **n4** (300 nM) was incubated with a 0.5% lipid solution (intralipid), as shown in Figure 3. Over the time course of the experiment (360 min), the fluorescence intensity increased 8-fold, corresponding to the release of 20% of the encapsulated porpholactol. Presumably, interactions between the lipid and the nanoparticles cause the porpholactol to leach into the surrounding media, minimizing the intermolecular quenching and allowing for an increase in the observed fluorescence intensity. This lipid-induced fluorescence enhancement is specific for the phorpholactol nanoparticles, **n4**, because it was not observed with the porphyrin nanoparticles, **n1**. On the basis of this hypothesis, the difference in polarity between porphyrin **1** and porpholactol **4** (the latter being more polar than porphyrin

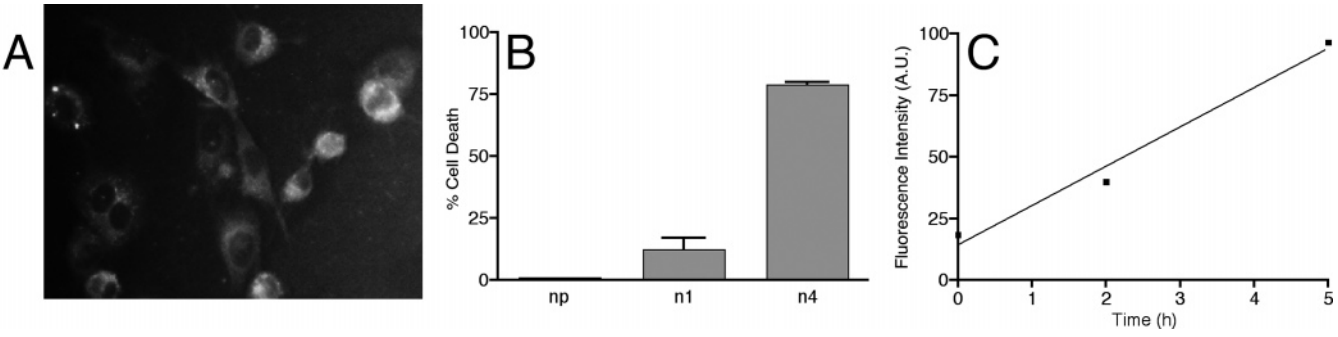

Figure 4. (A) Fluorescence microscopy image of 9L glioblastoma cells incubated for 1 h with **n4** nanoparticles. (B) Phototoxicity represented as percent of cell death after 3 h treatment with nanoparticles (10 μM) and illumination at 650 nm (42 mW cm^{-1}, 180 s). (C) Time-dependent increase in cell-associated fluorescence due to activation of internalized photosensitizer. Cells were treated with **n4** nanoparticles (10 μM) for 1 h, washed with media to remove noninternalized nanoparticles, and incubated for 0, 2, and 5 h. Background fluorescence intensity of control cells was 2.49.

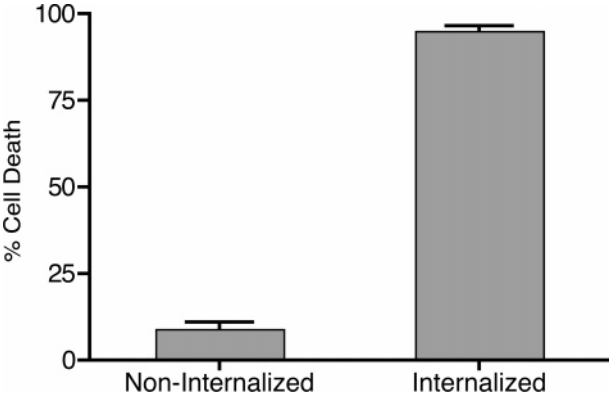

Figure 5. Comparative difference in phototoxicity between non-internalized and internalized **n4** nanoparticles (16 h treatment); identical concentration of **n4** in both experiments.

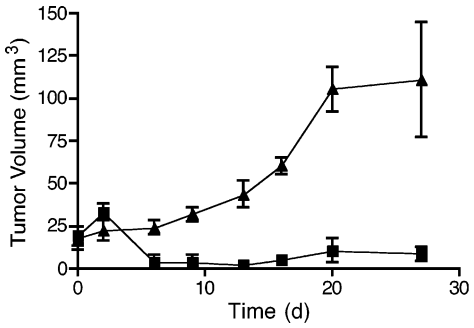

Figure 6. Comparison of tumor volume in untreated (▲) and treated (■) tumors over the time course of the experiment.

1) must be the cause of the preferential release and "activation" of **4** from the nanoparticle in the lipid solution.

Significantly, the specific lipid-induced release of **4** was also observed when cells were incubated with **n4** nanoparticles. FACS analysis of 9L glioblastoma, B16 melanoma, and BT breast carcinoma cells incubated with nanoparticles **n1** and **n4** for 1 h showed increased cellular fluorescence only for cells incubated with **n4** (Figure 4C). This finding was confirmed by fluorescence microscopy (Figure 4A), showing clear intracellular accumulation of **n4**, presumably in lysosomes.[17] No significant fluorescence was observed in cells treated with **n1**, as expected. The preferential release of porpholactol **4** from the nanoparticles (**n4**) also translated into selective phototoxicity in cultured cells (Figure 4B).

In another set of experiments, we determined the cellular toxicity of internalized versus external **n4** nanoparticles in cell culture. The photodynamic efficacy of **n4** (10 μM) in cells irradiated after incubation for 16 h was compared to that of cells that were treated with the same quantity and concentration of **n4** immediately prior to irradiation (Figure 5). The phototoxicity caused by the noninternalized nanoparticles (10 μM) is minimal (9% cell death), in contrast to the effect of internalized nanoparticles (95% cell death under identical testing conditions) (Figure 5). As expected, no effect was observed when **n1** was incubated with cells for 16 h.

The reduction in singlet oxygen generation of encapsulated versus free photosensitizer may be attributed to a number of different mechanisms. If aggregation within the particles causes almost complete quenching of the lowest singlet or triplet excited state of the molecule, then there will be no transfer of the triplet excited-state energy to ground-state molecular oxygen, therefore preventing the formation of cytotoxic singlet oxygen. Another possible explanation might

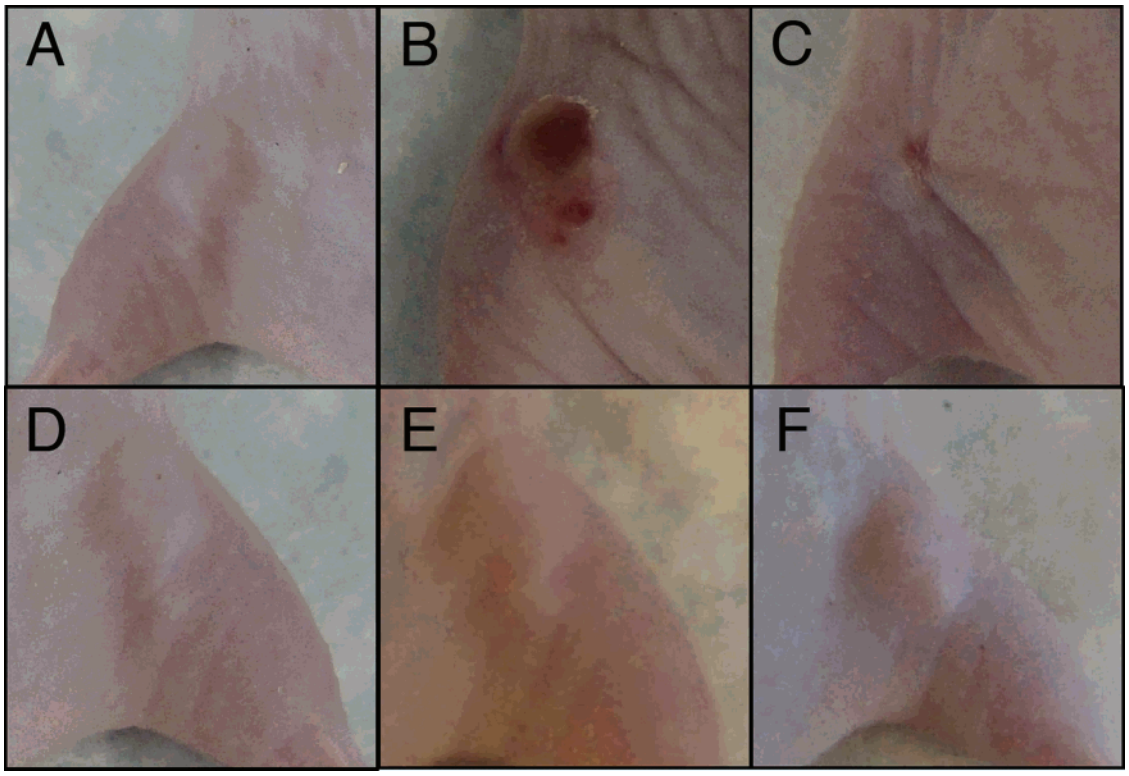

Figure 7. In vivo animal study. Treated Side: (A) day 0; (B) day 6; (C) day 27. Control side: (D) day 0; (E) day 6; (F) day 27.

be the inability of molecular oxygen to interact with the photosensitizer because the polymer acts as an impermeable barrier. Although others have reported the encapsulation of photosensitizers within PLGA, there was no mention of the latter occurring.[6a,b]

Finally, we performed in vivo animal studies in mouse models of cancer to ascertain the efficiency of the approach. Five nude mice were bilaterally implanted with prostate carcinoma cells via a subcutaneous injection into each flank. When the resulting tumors reached a palpable size (approximately 15 mm^3), nanoparticles were injected intravenously. Twenty-four hours later, animals were treated with light therapy administered to one flank only (191 mW/cm^2, 57.3 J/cm^2), while the opposite flank remained as an internal control. Tumor volume was monitored over the course of the study to determine the efficacy of the treatment (Figure 6).

Within 3 days of the phototherapy, local hemorrhaging was observed, which was followed by necrosis (Figure 7B). By day 27, all that remained at the tumor site was scarring (Figure 7C). Once the animals were sacrificed, tissue was removed from both the treated and untreated flanks and subject to histological examination (hematoxylin and eosin staining). On the untreated side, a large tumor is observed easily with a loose network of microvasculature and a well-defined capsule, whereas on the treated side the capsule has shrunken drastically and contained large amounts of collagen.

In summary, we have shown that the encapsulation of *meso*-tetraphenylporpholactol **4** results in nanoparticles containing a photosensitizer with quenched excited states that is released and activated upon cell internalization. This new nanoagent has several favorable properties for use as a photodynamic drug, including nontoxicity in extracellular spaces, and time-dependent intracellular release of the photosensitizer. The use of these activatable nanoparticles may result in a decrease in the amount of extraneous photosensitivity incurred because of nonspecific localization of the photosensitizer into healthy tissues or the skin. Furthermore, the use of a biodegradable polymer to synthesize the nanoparticles makes the final product attractive for clinical applications. This study opens up the potential for a new class of encapsulated nanomaterials with improved safety profiles, improved delivery, and dual imaging/therapeutic applications. Additional experimentation is currently being undertaken to further elucidate the photophysical and physiological properties of these nanoparticles.

Acknowledgment. We thank Peter Waterman for his assistance with the in vivo experimentation and Dr. Elena Aikawa-Rabkin for her assistance with the histology. This work was supported by NIH grant CA1010781 to J.M.P. and an NIH T32 Fellowship, CA79443 (R.W.), R01 HL080731 (R.W.), P50 CA86355 (R.W.).

Supporting Information Available: Synthesis and characterization of the nanoparticles, details of the experiments conducted, and histology. This material is available free of charge via the Internet at http://pubs.acs.org.

References

(1) (a) Dolmans, D. E.; Fukumura, D.; Jain, R. K. *Nat. Rev. Cancer* **2003**, *3*, 380−387. (b) Pandey, R. K.; Zheng, G. In *The Porphyrin Handbook*; Kadish, K. M., Smith, K. M., Guilard, R., Eds.; Academic Press: San Diego, 2000; Vol. 6, pp 157−230. (c) Sternberg, E. D.; Dolphin, D.; Brückner, C. *Tetrahedron* **1998**, *54*, 4151−4202.

(2) Gouterman, M. *J. Mol. Spectrosc.* **1961**, *6*, 138−163.

(3) Brückner, C.; McCarthy, J. R.; Daniell, H. W.; Pendon, Z. D.; Ilagan, R. P.; Francis, T. M.; Ren, L.; Birge, R. R.; Frank, H. A. *Chem. Phys.* **2003**, *294*, 285−303.

(4) Vrouenraets, M. B.; Visser, G. W.; Snow, G. B.; van Dongen, G. A. *Anticancer Res.* **2003**, *23*, 505−22.

(5) (a) Bisland, S. K.; Singh, D.; Gariépy, J. *Bioconjugate Chem.* **1999**, *10*, 982−992. (b) Chaloin, L.; Bigey, P.; Loup, C.; Marin, M.; Galeotti, N.; Piechaczyk, M.; Heitz, F.; Meunier, B. *Bioconjugate Chem.* **2001**, *12*, 691−700. (c) Del Governatore, M.; Hamblin, M. R.; Shea, C. R.; Rizvi, I.; Molpus, K. G.; Tanabe, K. K.; Hasan, T. *Cancer Res.* **2000**, *60*, 4200−4205. (d) Sharman, W. M.; van Lier, J. E.; Allen, C. M. *Adv. Drug. Deliv. Rev.* **2004**, *56*, 53−76. (e) van Dongen, G. A.; Visser, G. W.; Vrouenraets, M. B. *Adv. Drug. Deliv. Rev.* **2004**, *56*, 31−52. (f) Hudson, R.; Boyle, R. W. *J. Porphyrins Phthalocyanines* **2004**, *8*, 954−975.

(6) (a) Konan, Y. N.; Berton, M.; Gurny, R.; Allémann, E. *Eur. J. Pharm. Sci.* **2003**, *18*, 241−249. (b) Konan, Y. N.; Cerny, R.; Favet, J.; Berton, M.; Gurny, R.; Allémann, E. *Eur. J. Pharm. Biopharm.* **2003**, *55*, 115−124. (c) Roy, I.; Ohulchansky, T. Y.; Pudavar, H. E.; Bergey, E. J.; Oseroff, A. R.; Morgan, J.; Dougherty, T. J.; Prasad, P. N. *J. Am. Chem. Soc.* **2003**, *125*, 7860−7865. (d) Yan, F.; Kopelman, R. *Photochem. Photobiol.* **2003**, *78*, 587−591.

(7) (a) Bowers, P. G.; Porter, G. *Proc. R. Soc. London, Ser. A* **1967**, *296*, 435−441. (b) Heinzelmann, W.; Labhart, H. *Chem. Phys. Lett.* **1969**, *4*, 20−24. (c) Janot, J.-M.; Bienvenüe, E.; Seta, P.; Bensasson, R. V.; Tomé, A. C.; Enes, R. F.; Cavaliero, J. A. S.; Leach, S.; Camps, X.; Hirsch, A. *J. Chem. Soc., Perkin Trans. 2* **2000**, 301−306. (d) Segalla, A.; Borsarelli, C. D.; Braslavsky, S. E.; Spikes, J. D.; Roncucci, G.; Dei, D.; Chiti, G.; Jori, G.; Reddi, E. *Photochem. Photobiol. Sci.* **2002**, *1*, 641−648. (e) Tanielian, C.; Schweitzer, C.; Mechin, R.; Wolff, C. *Free Radical Biol. Med.* **2001**, *30*, 208−212.

(8) Maeda, H.; Seymour, L. W.; Miyamoto, Y. *Bioconjugate Chem.* **1992**, *3*, 351−362.

(9) Langer, R. *Nature* **1998**, *392*, 5−10.

(10) Brückner, C.; Rettig, S. J.; Dolphin, D. *J. Org. Chem.* **1998**, *63*, 2094−2098.

(11) McCarthy, J. R.; Jenkins, H. A.; Brückner, C. *Org. Lett.* **2003**, *5*, 19−22.

(12) Ntziachristos, V.; Tung, C.-H.; Bremer, C.;Weissleder, R. *Nat. Med.* **2002**, *8*, 757−761.

(13) Henderson, B. W.; Bellnier, D. A.; Greco, W. R.; Sharma, A.; Pandey, R. K.; Vaughan, L. A.; Weishaupt, K. R.; Dougherty, T. J. *Cancer Res.* **1997**, *57*, 4000−4007.

(14) (a) Harisinghani, M. G.; Barentsz, J.; Hahn, P. F.; Deserno, W. M.; Tabatabaei, S.; van de Kaa, C. H.; de la Rosette, J.; Weissleder, R. *N. Engl. J. Med.* **2003**, *348*, 2491−2499. (b) Perez, J. M.; Simeone, F. J.; Saeki, Y.; Josephson, L.; Weissleder, R. *J. Am. Chem. Soc.* **2003**, *125*, 10192−10193.

(15) Bourdon, O.; Mosqueira, V.; Legrand, P.; Blais, J. *J. Photochem. Photobiol., B* **2000**, *55*, 164−171.

(16) (a) Hunter, C. A.; Sanders, J. K. M. *J. Am. Chem. Soc.* **1990**, *112*, 5525−5534. (b) Hunter, C. A.; Sanders, J. K. M.; Stone, A. *J. Chem. Phys.* **1989**, *133*, 395−404. (c) Kasha, M. *Radiat. Res.* **1963**, *20*, 55−70.

(17) Panyam, J.; Zhou, W.-Z.; Prabha, S.; Sahoo, S. K.; Labhasetwar, V. *FASEB J.* **2002**, *16*, 1217−1226.

NL0519229